

Increased *CYP2J3* Expression Reduces Insulin Resistance in Fructose-Treated Rats and *db/db* Mice

Xizhen Xu,¹ Chun Xia Zhao,¹ Luyun Wang,¹ Ling Tu,¹ Xiaosai Fang,¹ Changlong Zheng,¹ Matthew L. Edin,² Darryl C. Zeldin,² and Dao Wen Wang¹

OBJECTIVE—Accumulating evidence suggests that cytochrome P450 (CYP) epoxygenases metabolize arachidonic acid into epoxyeicosatrienoic acids (EETs), which play crucial and diverse roles in cardiovascular homeostasis. The anti-inflammatory, antihypertensive, and pro-proliferative effects of EETs suggest a possible beneficial role for EETs on insulin resistance and diabetes.

RESEARCH DESIGN AND METHODS—This study investigated the effects of *CYP2J3* epoxygenase gene therapy on insulin resistance and blood pressure in diabetic *db/db* mice and in a model of fructose-induced hypertension and insulin resistance in rats.

RESULTS—*CYP2J3* gene delivery in vivo increased EET generation, reduced blood pressure, and reversed insulin resistance as determined by plasma glucose levels, homeostasis model assessment insulin resistance index, and glucose tolerance test. Furthermore, *CYP2J3* treatment prevented fructose-induced decreases in insulin receptor signaling and phosphorylation of AMP-activated protein kinases (AMPKs) in liver, muscle, heart, kidney, and aorta. Thus, overexpression of *CYP2J3* protected against diabetes and insulin resistance in peripheral tissues through activation of insulin receptor and AMPK pathways.

CONCLUSIONS—These results highlight the beneficial roles of the CYP epoxygenase-EET system in diabetes and insulin resistance. *Diabetes* 59:997–1005, 2010

Arachidonic acid is liberated from cell membranes by phospholipases in response to various stimuli and is subsequently metabolized by three different enzyme pathways, namely the cyclooxygenase, the lipoxygenase, and the cytochrome P450 (CYP) epoxygenase pathways. Metabolism of arachidonic acid via CYP epoxygenases produces four different *cis*-epoxyeicosatrienoic acids (EETs): 5,6-, 8,9-, 11,12-, and 14,15-EET. Human P450 2J2 (CYP2J2) and its rat homolog CYP2J3 are predominant enzymes responsible for the oxidation of endogenous arachidonic acid pools in cardiac myocytes, vascular endothelium, pancreas, and other tis-

sues where they exert regulatory effects in normal and pathophysiological processes (1–4).

Accumulating evidence suggests that EETs play crucial and diverse roles in cardiovascular homeostasis. Arachidonic acid epoxygenase metabolites stimulate endothelial cell growth and angiogenesis via mitogen-activated protein kinase (MAPK) and phosphatidylinositol 3-kinase (PI 3-kinase)/AKT signaling pathways, and to some extent, the endothelial NO synthase (eNOS) pathway (5). Moreover, EETs upregulate eNOS in bovine aortic endothelial cells via activation of MAPK, protein kinase C, PI 3-kinase/AKT, and MAPK signaling pathways (6,7). CYP epoxygenase overexpression, which increases EET biosynthesis, significantly protects endothelial cells from apoptosis induced by tumor necrosis factor- α (TNF- α), an effect that is mediated, at least in part, through inhibition of MAPK dephosphorylation and activation of PI 3-kinase/AKT pathways (8). Furthermore, CYP-derived eicosanoids are vasodilatory, at least in part through their ability to activate eNOS and NO release (9).

Considerable experimental evidence suggests that eNOS-derived NO is a pivotal regulator of blood pressure, vascular tone, and vascular homeostasis (10–14). Experimental evidence also suggests that NO is involved in the pathogenesis of diabetes and insulin resistance. NADPH oxidases in the vascular wall are activated in diabetes, leading to enhanced degradation of NO and the production of reactive oxygen species (15). Uncoupling of eNOS has been demonstrated in animal models of diabetes (16), and endogenous NO synthase inhibitors including asymmetric dimethylarginine are an important cause of vascular insulin resistance (17). Cumulatively, these data indicate that diabetes and insulin resistance are characterized, to some degree, by endothelial dysfunction, altered eNOS expression, and NO production. Insulin mediates its effects through binding to insulin receptors and triggering downstream signaling pathways, of which the most important is the PI 3-kinase/AKT pathway. This pathway is involved in a variety of insulin responses including protection from apoptosis and transport of glucose through cell membranes in endothelial cells (8,18).

We hypothesized that overexpression of *CYP2J3* and the subsequent increase in production of EETs might be beneficial in attenuating hypertension and insulin resistance. Thus, the present study investigated the effects and underlying mechanisms of *CYP2J3* gene therapy on insulin resistance and diabetes in fructose-induced insulin resistance in rats and in diabetic *db/db* mice.

RESEARCH DESIGN AND METHODS

Materials and reagents. Materials were obtained from the following suppliers: Antibodies involved in this study were from Santa Cruz Biotechnology (Santa Cruz, CA); the rabbit polyclonal anti-CYP2J3 antibody was developed in our laboratory as described (4); fructose, glucose, triglyceride, and chole-

From the ¹Department of Internal Medicine and The Institute of Hypertension, Tongji Hospital, Tongji Medical College of Huazhong University of Science and Technology, Wuhan, People's Republic of China; and the ²Division of Intramural Research, National Institute of Environmental Health Sciences, National Institutes of Health, Research Triangle Park, North Carolina. Corresponding author: Dao Wen Wang, dwwang@tjh.tjmu.edu.cn. Received 27 August 2009 and accepted 21 December 2009. Published ahead of print at <http://diabetes.diabetesjournals.org> on 12 January 2010. DOI: 10.2337/db09-1241.

X.X., C.X.Z., and L.W. contributed equally to this study.

© 2010 by the American Diabetes Association. Readers may use this article as long as the work is properly cited, the use is educational and not for profit, and the work is not altered. See <http://creativecommons.org/licenses/by-nc-nd/3.0/> for details.

The costs of publication of this article were defrayed in part by the payment of page charges. This article must therefore be hereby marked "advertisement" in accordance with 18 U.S.C. Section 1734 solely to indicate this fact.

terol reagents were from Ningbo Cicheng Biocompany (Ningbo, China); Rat/Mouse Insulin ELISA Kit was from Linco Research (St. Charles, MO); 14,15-DHET ELISA Kit was from Detroit R&D (Detroit, MI); and guanosine 3',5'-cyclic monophosphate (cGMP) and cAMP ELISA kit was from Cayman Chemical (Ann Arbor, MI). All other chemicals and reagents were purchased from Sigma-Aldrich unless otherwise specified. Full-length *CYP2J3* cDNA was cloned from rat liver RNA and then subcloned into the pcDNA plasmid vector in sense (*CYP2J3*⁺) and antisense (*CYP2J3*⁻) orientations.

Animals. All animal experimental protocols complied with standards stated in the National Institutes of Health *Guidelines for the Care and Use of Laboratory Animals* and were approved by The Academy of Sciences of China. Male Sprague-Dawley rats weighing 200 ± 20 g and male C57BL/6 and *db/db* mice (8 weeks old) were obtained from the Experimental Animal Center of Shanghai (Shanghai, People's Republic of China). Animals were treated before experiments as described previously (19).

Fructose feeding and gene delivery protocols. After a 1-week adaptation period (i.e., beginning at week 0), rats were fed normal rat chow and either normal water ($n = 32$) or water containing 10% fructose ($n = 24$) for a total of 5 weeks. Systolic blood pressure was measured weekly until week 6, and gene delivery protocols were undertaken at week 3 as described previously (19).

For the mouse study, C57BL/6 and *db/db* mice were anesthetized with diethyl ether and received a sublingual vein injection of plasmid at a dose of 5 mg/kg body wt. C57BL/6 mice received either empty pcDNA (C57BL/6 + pcDNA), *CYP2J3*⁺ (C57BL/6 + *CYP2J3*⁺), or 0.9% NaCl (C57BL/6 normal) ($n = 8$ per group), and *db/db* mice similarly received either pcDNA (*db/db* + pcDNA), *CYP2J3*⁺ (*db/db* + *CYP2J3*⁺), or 0.9% NaCl (*db/db* normal) ($n = 8$ per group).

Blood pressure measurement. Systolic blood pressure was measured weekly in conscious rats with a manometer-tachometer (Rat Tail NIBP System; ADI Instruments, Bella Vista, NSW, Australia) using the tail-cuff method as described previously (19).

Rat serum and urine analyses. Serum and urine samples from all rats were collected. Fasting serum levels of insulin, glucose, sodium, potassium, magnesium, cholesterol, triglycerides, LDL cholesterol, and HDL cholesterol as well as urine levels of sodium, potassium, and magnesium were assessed as described previously (19). Similarly, serum and urine samples from all mice were collected, and serum levels of insulin, glucose, cholesterol, triglycerides, LDL cholesterol, and HDL cholesterol were assessed. Serum levels of alanine aminotransferase, urea, and creatinine in rats were also measured on an AEROSSET Clinical Chemistry System (Abbott Laboratories) to evaluate renal and liver function. Additional details are provided in the supplementary methods, available in an online appendix at <http://diabetes.diabetesjournals.org/cgi/content/full/db09-1241/DC1>.

Glucose tolerance test. At 2 weeks after gene delivery, C57BL/6 and *db/db* mice were fasted overnight (for 16 h) and then injected intraperitoneally with D-glucose (20% solution; 2 g/kg body wt). At 0, 30, 60, and 120 min after glucose administration, blood samples were taken from the cavernous sinus with a capillary while under ether anesthesia. Plasma glucose and insulin levels were determined using methods identical to those used for serum samples in rats (described in detail in the online supplementary methods).

Evaluation of urine 14,15-DHET by ELISA. To assess in vivo EET production, an ELISA kit (Detroit R&D) was used to determine concentrations of the stable EET metabolite 14,15-dihydroxyeicosatrienoic acid (14,15-DHET) in the urine of rats and mice. 14,15-DHET was quantified by enzyme-linked immunosorbent assay (ELISA) according to the manufacturer's instructions, as previously described (7).

RT-PCR analysis of aortic ET-1 and ETA-R mRNA. Total RNA was extracted from frozen rat aortas using TRIZOL reagent (Invitrogen, Carlsbad, CA) and used to assess mRNA levels of ET-1 and ETA-R. The following oligonucleotide primers were used for amplification of the ET-1 and ETA-R cDNAs from reverse-transcribed aortic RNA: ET-1 (forward): 5'-AAGCGTTGCTCTGCTCCTCC-3'; ET-1 (reverse): 5'-TTCCCTGGTCTGGTCTTTGTG-3'; ETA-R (forward): 5'-TGCTCAACGCCACGACCAAGT-3'; ETA-R (reverse): 5'-GGTGTTCGCTGAGGCAATCC-3'.

Amplification was performed on an ABI7500 PCR system (Applied Biosystems, Darmstadt, Germany) after incubation with Moloney murine leukemia virus reverse transcriptase at 42°C for 15 min. A preheating step of 5 min at 95°C was followed by 40 cycles consisting of 30 s at 95°C, 20 s at 60°C, and 20 s at 72°C. PCR products were electrophoresed on 1.5% agarose gels. The quantities of specific ET-1 and ETA-R transcripts were normalized to levels of glyceraldehyde-3-phosphate dehydrogenase transcripts to control for RNA quality and amount.

Western blot analysis. At 2 weeks after gene injection, rats and mice from each group were anesthetized with pentobarbital (100 mg/kg i.p.), and skeletal muscles, aortas, hearts, kidneys, and livers were excised, frozen in liquid nitrogen, and stored at -80°C. Western blotting was performed as described previously (19). Expression was quantified by densitometry and normalized to β -actin

TABLE 1

Physiological parameters determined in rats after 3 weeks of administration of control or fructose-containing drinking water

Variables	Control group ($n = 32$)	Fructose-treated group ($n = 24$)
Glucose (mmol/l)	4.91 ± 0.2	5.62 ± 0.4
Triglycerides (mmol/l)	0.45 ± 0.12	$1.18 \pm 0.47^*$
Insulin (mIU/l)	17.74 ± 0.59	$49.11 \pm 0.42^*$
HOMA-IR	4.21 ± 0.56	$14.24 \pm 0.86^\dagger$
Body weight (g)	254 ± 33	267 ± 26

Physiological parameters determined in rats after 3 weeks of administration of normal or fructose-containing drinking water. Fasting triglyceride, insulin levels, and HOMA-IR were increased in fructose-treated rats after 3 weeks of administration of fructose-containing drinking water. Values shown are mean \pm SE from each group of rats, respectively. * $P < 0.05$, $^\dagger P < 0.001$ compared with rats treated with water.

expression. All groups were then normalized to their respective controls, and bar graphs represent quantification of at least three independent experiments.

Evaluation of urinary cAMP and cGMP by ELISA. Urinary cAMP and cGMP levels were measured by ELISA as previously described (20,21).

Statistical analysis. Continuous data were expressed as means \pm SEM. Comparisons between groups were performed by a one-way ANOVA. Two-way ANOVA was used to examine differences in response to treatments and between groups, with post hoc analyses performed using the Student-Newman-Keuls test. Statistical significance was defined as $P < 0.05$.

RESULTS

Blood pressure and metabolic changes in fructose-treated rats. All rats in the study were assessed for a variety of physiological parameters 3 weeks after receiving either control or fructose-containing drinking water. As expected, consumption of fructose-containing water resulted in significantly increased systolic blood pressure, significantly increased levels of serum insulin, serum triglyceride, urine potassium, urine magnesium, and urine volume, and significantly decreased urine osmolarity (all $P < 0.05$) (Table 1, Fig. 1, and supplementary Table 1). Homeostasis model assessment insulin resistance (HOMA-IR) also was significantly increased in fructose-treated rats ($P < 0.05$) (Table 1). These data indicate that fructose administration induced hypertension, insulin resistance, and hypo-osmolar diuresis as described previously (19).

Effects of *CYP2J3* gene delivery on *CYP2J3* protein expression and on fructose-induced hypertension and pathophysiological changes in rats. At 2 weeks after gene delivery (i.e., at week 5 of the study), *CYP2J3* protein levels were increased in the aorta, heart, liver, and kidney of fructose-treated *CYP2J3*⁺ (F + *CYP2J3*⁺) rats compared with fructose-treated rats injected with *CYP2J3*⁻ or with the empty pcDNA vector (Fig. 1A). Importantly, *CYP2J3* functionality was demonstrated by the nearly four-fold increase in urinary 14,15-DHET levels in rats injected with *CYP2J3*⁺ compared with those injected with *CYP2J3*⁻ or with the empty pcDNA vector (Fig. 1B).

Injection of *CYP2J3*⁺ to fructose-treated rats resulted in decreased systolic blood pressure 1, 2, and 3 weeks after injection (i.e., at weeks 4, 5, and 6 of the study, respectively) compared with that observed in fructose-treated rats injected with the control pcDNA or *CYP2J3*⁻ vectors (Fig. 1C). The maximum reduction in blood pressure in F + *CYP2J3*⁺ rats was observed 2 weeks after injection (i.e., at week 5 of the study) when blood pressure reached a level similar to those observed in rats drinking normal water (Fig. 1C). No changes in blood pressure compared

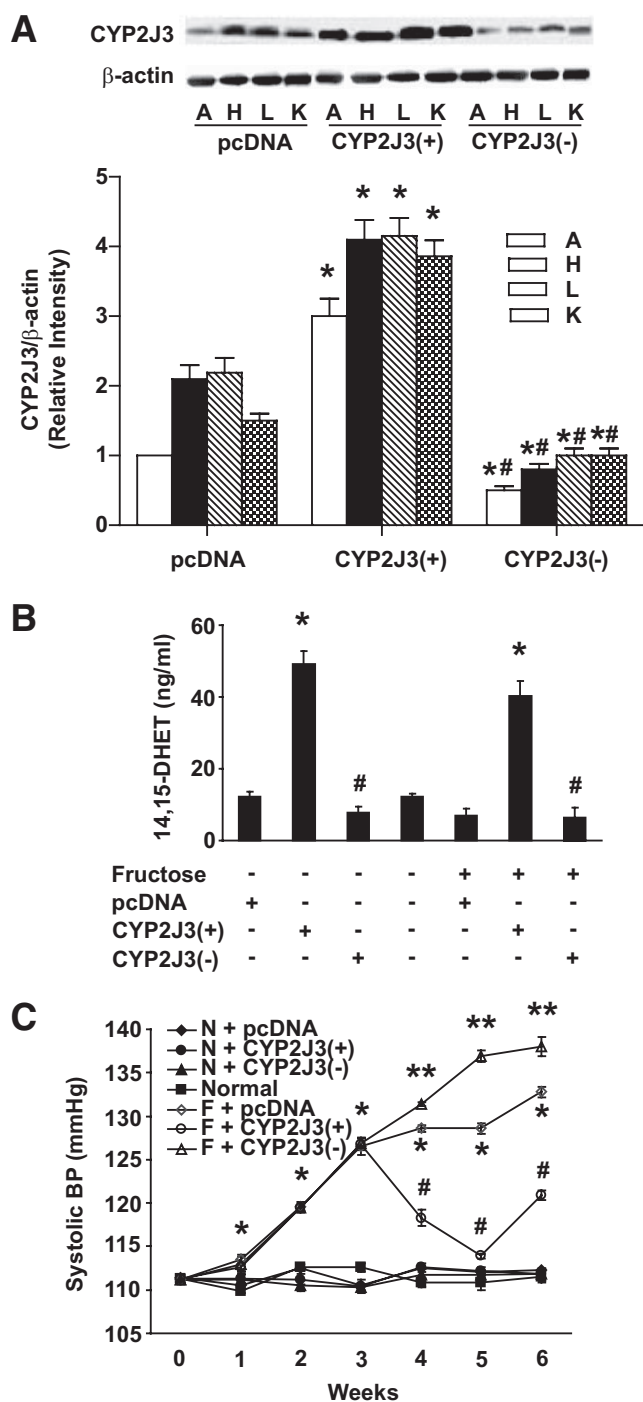


FIG. 1. Effects of *CYP2J3* gene delivery on *CYP2J3* protein expression, urinary 14,15-DHET levels, and fructose-induced hypertension in rats. **A:** *CYP2J3* protein levels were increased in aorta (A), heart (H), liver (L), and kidney (K) of fructose-treated rats 2 weeks after injection of *CYP2J3*⁺ but not after injection of *CYP2J3*⁻ or empty vector (pcDNA). **B:** Urinary 14,15-DHET levels were increased in control and fructose-treated rats injected with *CYP2J3*⁺ compared with rats injected with *CYP2J3*⁻ or empty vector (pcDNA). **P* < 0.01 versus pcDNA; #*P* < 0.01 versus *CYP2J3*⁺; *n* = 8 per group. **C:** The elevation of systolic blood pressure (BP) observed in fructose-treated rats was decreased 1, 2, and 3 weeks after injection of *CYP2J3*⁺ (i.e., at weeks 4, 5, and 6 of the study, respectively) but not after injection with *CYP2J3*⁻ or empty vector (pcDNA). Values shown are mean ± SEM from each group of rats. **P* < 0.01 compared with rats treated without fructose, #*P* < 0.01 compared with rats treated with fructose, ***P* < 0.01 compared with rats treated with *CYP2J3*⁺; *n* = 4–10 per group per time point.

with saline-injected rats were observed in normal drinking water-treated rats administered pcDNA, *CYP2J3*⁺, or *CYP2J3*⁻ (Fig. 1C). These data indicate that *CYP2J3* overexpression reduced hypertension in fructose-treated rats but had no effect on blood pressure in normal control rats.

Other physiological and biochemical parameters related to hypertension and hyperinsulinemia were assessed in eight rats per experimental group 2 weeks after gene delivery (week 5) (Table 2 and supplementary Table 2). Compared with values in the normal water-treated groups, serum insulin, insulin resistance (HOMA-IR), serum triglycerides, urine volume, urine potassium, and urine magnesium levels were all higher, whereas urine osmolarity was lower in fructose-treated rats injected with the empty pcDNA vector (F + pcDNA group; all *P* < 0.05) (Table 2 and supplementary Table 2). With the exception of serum triglyceride levels, all of these changes were prevented by injection of fructose-treated rats with *CYP2J3*⁺, but not with *CYP2J3*⁻ (Table 2 and supplementary Table 2). These data indicate that *CYP2J3* overexpression markedly attenuated fructose-induced insulin resistance in rats but that it had no effect on these parameters in normal water-treated rats.

Compared with values in the normal water-treated groups, serum alanine aminotransferase, urea nitrogen, and creatinine showed no significant changes in fructose-treated rats injected with the empty pcDNA vector (F + pcDNA group; all *P* > 0.05). Compared with values in rats injected with empty pcDNA vector, serum alanine aminotransferase, urea nitrogen, and creatinine were not significantly changed in rats injected with *CYP2J3*⁺ (supplementary Table 3). These data indicate that *CYP2J3* overexpression has no detrimental effects on rat renal and liver function.

Effects of *CYP2J3* gene delivery on rat insulin receptor signaling and eNOS, ET-1, and ETA-R expression. PI 3-kinase is recruited to insulin receptor substrate (IRS) signaling complexes through binding of Src homology 2 domains in its 85-kDa regulatory subunit to specific phosphotyrosine residues in IRS-1, a process that leads to activation of the PI 3-kinase p110 catalytic subunit (22). To investigate the signaling mechanisms through which *CYP2J3* attenuates fructose-induced insulin resistance, we evaluated the expression of IRS-1 associated with the insulin signaling cascade in rat liver and skeletal muscle. Compared with levels in normal control rats, fructose drinking resulted in significantly decreased IRS-1 levels in liver and skeletal muscle (Fig. 2A and B). Phospho-Y989-IRS-1 levels were similarly decreased in liver and skeletal muscle, whereas phospho-S307-IRS-1 was significantly increased (supplementary Fig. 1A and B). Administration of *CYP2J3*⁺ significantly reversed the changes in IRS-1 and phospho-IRS-1 levels induced by fructose in both liver and skeletal muscle (Fig. 2A and B; supplementary Fig. 1A and B).

Compared with expression in corresponding control animals, eNOS protein expression was downregulated in aorta, liver, and skeletal muscle in fructose-treated rats; this effect was not observed in fructose-treated rats injected with *CYP2J3*⁺ (Fig. 2C; supplementary Fig. 1C and D). Similar changes in eNOS expression and effects of *CYP2J3*⁺ were observed in rat heart and kidney (data not shown). These data suggest that *CYP2J3*⁺ treatment restored eNOS activity and support previous observations of a beneficial effect of eNOS against fructose-induced hypertension and hyperinsulinemia (23).

The expression of ET-1 and ETA-R mRNA transcripts in

TABLE 2

Physiological parameters determined in rats 2 weeks after injection of empty pcDNA3.1 vector, pcDNA-2J3⁺, or pcDNA-2J3⁻

Variables	Treatment group						
	Normal water treated			Normal	Fructose treated		
	N + pcDNA3.1	N + p2J3 ⁺	N + p2J3 ⁻		F + pcDNA3.1	F + p2J3 ⁺	N + p2J3 ⁻
Glucose (mmol/l)	5.36 ± 0.68	6.99 ± 0.06	5.69 ± 0.86	5.09 ± 0.36	6.55 ± 0.58	6.44 ± 0.68	6.85 ± 0.99
Triglycerides (mmol/l)	0.61 ± 0.22	0.63 ± 0.39	0.45 ± 0.18	0.53 ± 0.09	1.04 ± 0.89*	1.30 ± 0.13	1.26 ± 0.4
Insulin (mIU/l)	22.65 ± 0.94	18.16 ± 0.81	18.83 ± 0.44	20.5 ± 0.64	49.71 ± 0.71*	19.48 ± 0.18†	60.25 ± 0.08‡
HOMA-IR	5.26 ± 0.82	4.16 ± 0.36	6.64 ± 0.61	5.06 ± 0.26	14.25 ± 0.02*	5.40 ± 0.59†	24.28 ± 0.04‡
Body weight (g)	310 ± 34	311 ± 49	307 ± 35	299 ± 40	297 ± 49	303 ± 31	341 ± 65

Compared with values in the normal water-treated groups, serum insulin, insulin resistance (HOMA-IR), and serum triglycerides levels were all higher in fructose-treated rats injected with the empty pcDNA vector (F + pcDNA group). With the exception of serum triglyceride levels, all of these changes were prevented by injection of fructose-treated rats with CYP2J3⁺ but not CYP2J3⁻. **P* < 0.05 vs. N + pcDNA3.1 group; †*P* < 0.05 vs. F + pcDNA3.1 group; ‡*P* < 0.05 vs. F + p2J3⁺ group; *n* = 8 per group.

rat aortas was determined by RT-PCR 2 weeks after gene delivery to examine the effects of fructose feeding and CYP2J3 gene delivery on the endothelin pathway, which has been shown to play a role in blood pressure homeostasis. Fructose administration resulted in significant increases in aortic ET-1 and ETA-R mRNA levels (Fig. 2D and E). These changes were prevented in rats administered CYP2J3⁺, but not in rats administered CYP2J3⁻.

Effects of CYP2J3 gene delivery on CYP2J3 protein expression and on pathophysiological changes and glucose tolerance in db/db mice. Similar to observations in fructose-fed rats, levels of CYP2J3 protein were increased in the aorta, heart, liver, and kidney in diabetic db/db mice 2 weeks after injection with CYP2J3⁺ compared with levels observed after injection with the empty pcDNA vector (Fig. 3A). Functionality of the CYP2J3

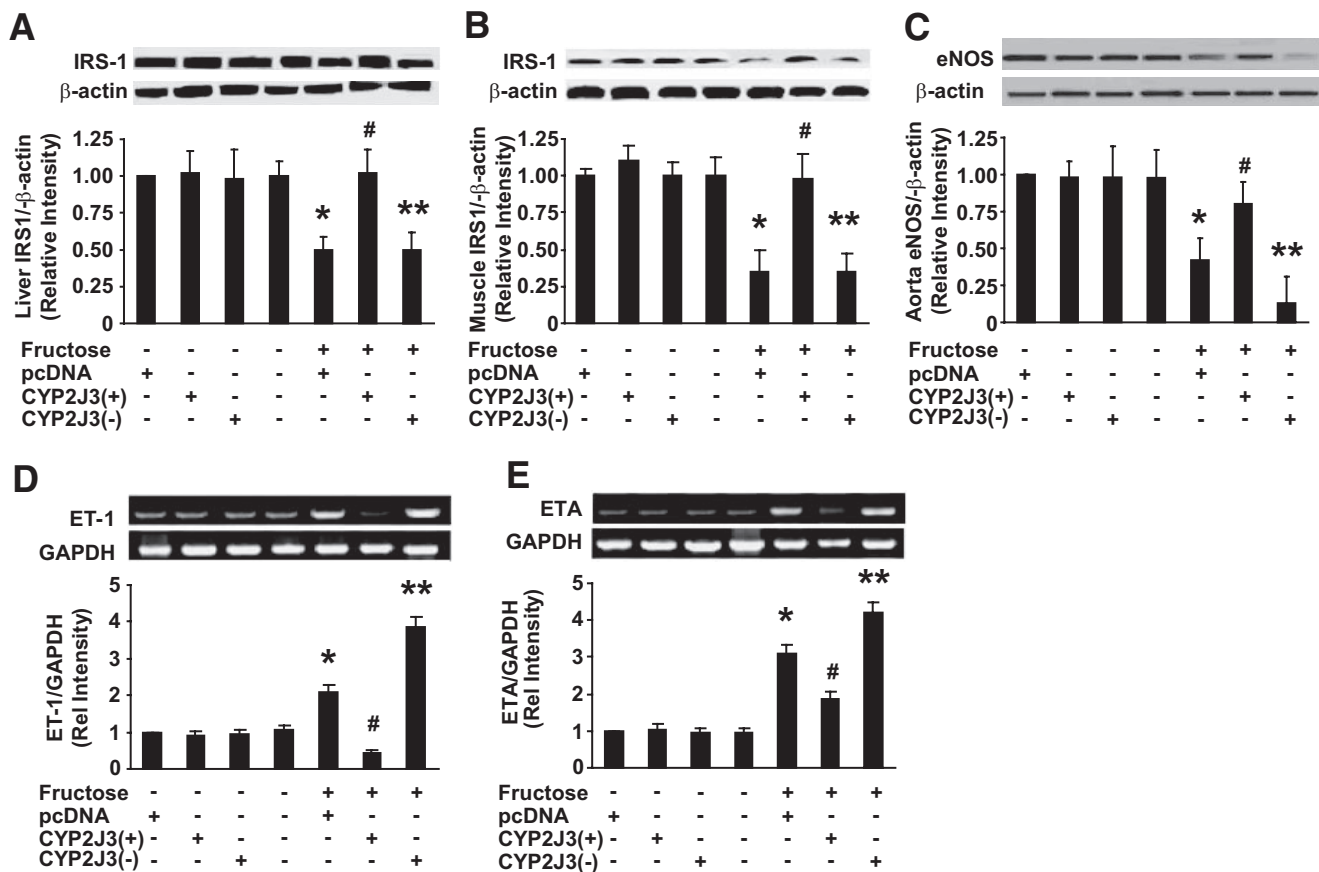


FIG. 2. Expression of IRS-1, eNOS, ET-1, and ETA-R in fructose-treated rats. Fructose administration to rats resulted in significantly decreased IRS-1 protein levels in liver (A) and skeletal muscle (B) and significantly decreased eNOS protein levels in aorta (C). These effects were inhibited by injection of CYP2J3⁺, but not by injection of CYP2J3⁻. Representative Western blots are shown above graphs summarizing densitometric quantification. **P* < 0.05 versus N + pcDNA; #*P* < 0.05 versus F + pcDNA; ***P* < 0.05 versus F + CYP2J3⁺; *n* = 8 per group. Levels of ET-1 (D) and ETA-R (E) transcripts relative to glyceraldehyde-3-phosphate dehydrogenase were assessed by RT-PCR in aortic tissue samples from three rats from each treatment group at week 5 of the study. Representative RT-PCR of ET-1 or ETA-R mRNA expression and corresponding densitometric quantification of three experiments are shown. Values shown are mean ± SEM. **P* < 0.05 versus N + pcDNA3.1; #*P* < 0.05 versus F + pcDNA3.1; ***P* < 0.05 versus F + pcDNA-CYP2J3⁺. Effects of CYP2J3 gene delivery on rat insulin receptor signaling and eNOS expression. Fructose administration to rats resulted in significantly decreased eNOS protein levels in aorta (C) and decreased IRS-1 protein levels in liver (D) and skeletal muscle (E). These effects were inhibited by injection of CYP2J3⁺, but not by injection of CYP2J3⁻. Representative Western blots are shown above graphs summarizing densitometric quantification. **P* < 0.05 versus N + pcDNA; #*P* < 0.05 versus F + pcDNA; ***P* < 0.05 versus F + CYP2J3⁺; *n* = 8 per group.

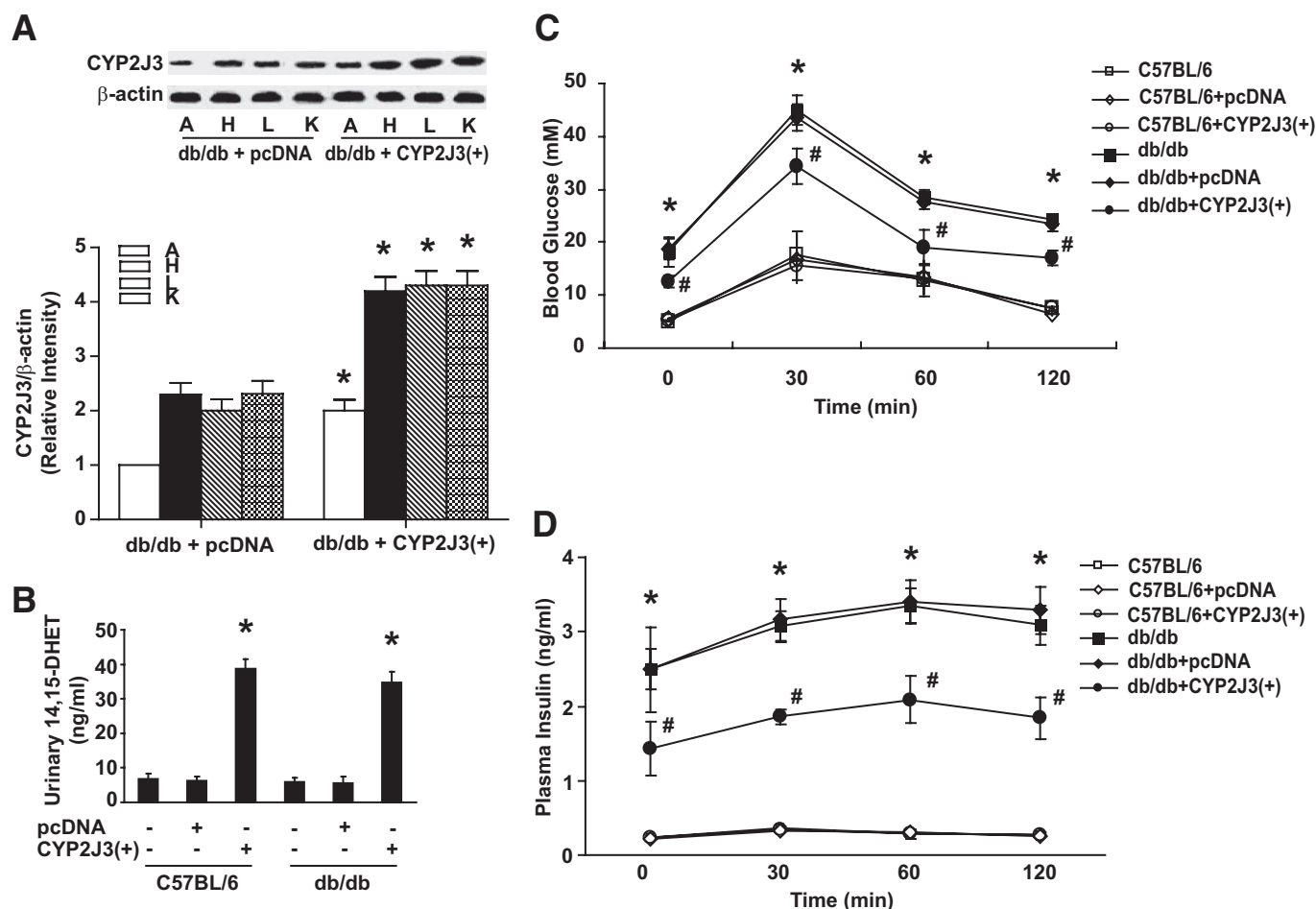


FIG. 3. Effects of *CYP2J3* gene delivery on *CYP2J3* protein expression, urinary 14,15-DHET levels, and glucose tolerance in *db/db* mice. **A:** Levels of *CYP2J3* protein were increased in the aorta (A), heart (H), liver (L), and kidney (K) in diabetic *db/db* mice 2 weeks after injection with *CYP2J3*⁺ compared with levels observed after injection with the empty pcDNA vector. **B:** Urinary 14,15-DHET levels were increased in C57BL/6 and *db/db* mice injected with *CYP2J3*⁺ compared with those injected with the empty pcDNA vector. **P* < 0.05 versus control and pcDNA-treated mice of corresponding genotype; *n* = 8 per group. Blood glucose (**C**) and plasma insulin (**D**) levels before and up to 120 min after a single glucose challenge were elevated in *db/db* mice and decreased by injection with *CYP2J3*⁺. No such reduction was observed in *db/db* mice injected with empty vector (pcDNA). **P* < 0.05 versus C57BL/6; #*P* < 0.05 versus *db/db* + pcDNA; *n* = 8 per group.

protein in *db/db* mice was demonstrated by the nearly fivefold increase in urinary 14,15-DHET levels in both C57BL/6 and *db/db* mice injected with *CYP2J3*⁺ compared with those injected with the empty pcDNA vector (Fig. 3B).

The diabetic phenotype of *db/db* mice (injected with the empty pcDNA vector) was confirmed by significantly higher levels of serum glucose, serum insulin, insulin

resistance (HOMA-IR), serum triglycerides, serum cholesterol, and urine volume in these animals compared with those in C57BL/6 mice (all *P* < 0.05; Table 3 and supplementary Table 4). Injection of *CYP2J3*⁺ significantly reduced insulin resistance (HOMA-IR) and urine volume in *db/db* mice, whereas injection of the empty pcDNA vector did not (Table 3 and supplementary Table 4). Although not all parameters of the diabetic phenotype in *db/db* mice

TABLE 3
Physiological parameters determined in mice 2 weeks after injection of empty pcDNA3.1 vector or pcDNA-2J3⁺

Variables	C57BL/6	C57BL/6 + pcDNA3.1	C57BL/6 + p2J3 ⁺	<i>db/db</i>	<i>db/db</i> + pcDNA3.1	<i>db/db</i> + p2J3 ⁺
Glucose (mmol/l)	10.48 ± 0.57	9.78 ± 0.38	9.70 ± 0.60	21.99 ± 1.83*	23.19 ± 2.51*	23.15 ± 2.36
Triglycerides (mmol/l)	1.2 ± 0.15	1.5 ± 0.22	1.43 ± 0.14	2.26 ± 0.28*	2.63 ± 0.00.32*	2.57 ± 0.37
Insulin (mIU/l)	2.06 ± 0.35	2.13 ± 0.36	1.46 ± 0.31	7.66 ± 1.33*	7.25 ± 0.87*	8.25 ± 1.96
Fasting glucose (mmol/l)	5.54 ± 0.33	5.67 ± 0.26	5.18 ± 0.40	17.52 ± 3.20*	18.80 ± 2.35*	12.65 ± 1.14†
Fasting insulin (ng/ml)	0.23 ± 0.02	0.22 ± 0.03	0.23 ± 0.01	2.49 ± 0.57*	2.618 ± 0.19*	1.43 ± 0.36†
HOMA-IR	0.053 ± 0.006	0.055 ± 0.005	0.052 ± 0.002	2.19 ± 0.72*	2.26 ± 0.45*	0.81 ± 0.24†
Body weight (g)	25.48 ± 0.61	25.45 ± 0.68	25.27 ± 0.47	45.16 ± 0.91	45.06 ± 0.97	45.78 ± 1.57

Serum glucose, serum insulin, insulin resistance (HOMA-IR), and serum triglyceride levels were significantly higher in the diabetic phenotype of *db/db* mice (injected with the empty pcDNA vector) compared with those in C57BL/6 mice. Injection of *CYP2J3*⁺ significantly reduced insulin resistance (HOMA-IR) in *db/db* mice, whereas injection of the empty pcDNA vector did not. **P* < 0.05 vs. C57BL/6 group; †*P* < 0.05 vs. *db/db* + pcDNA3.1 group; *n* = 8 per group.

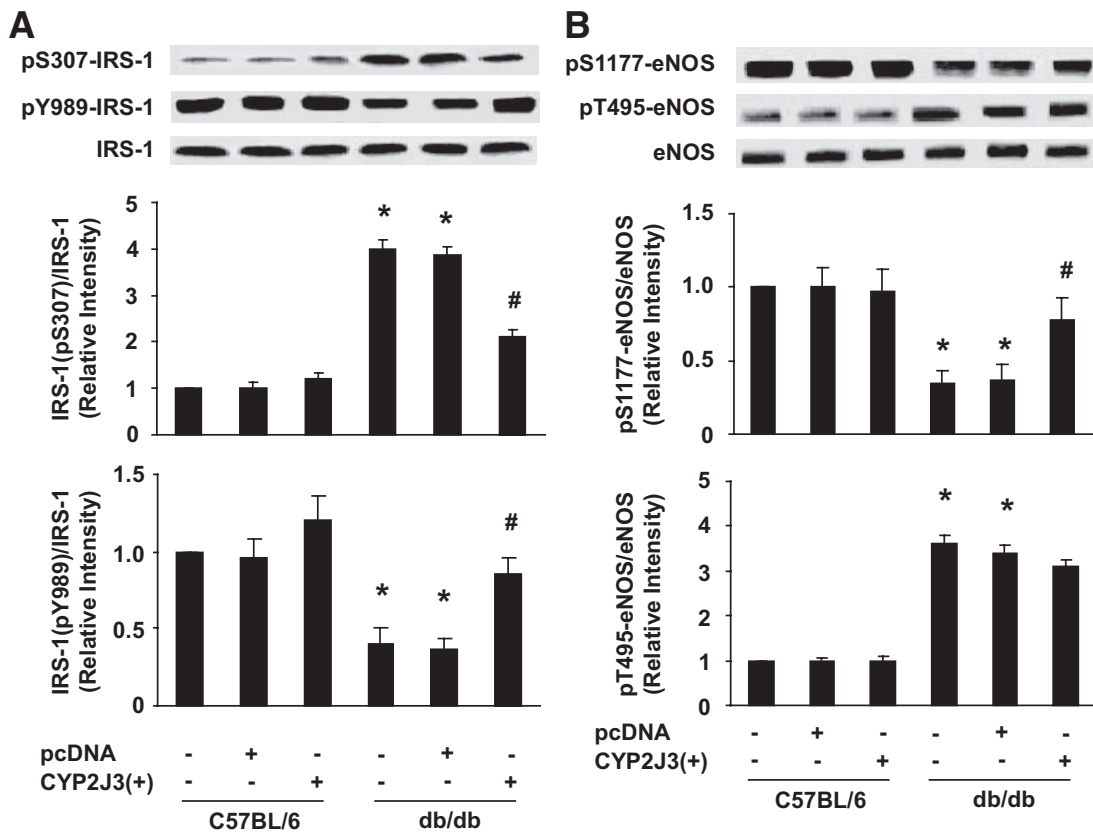


FIG. 4. Effects of *CYP2J3* gene delivery on activation of mouse insulin receptor signaling and eNOS phosphorylation. **A:** Relative to levels in C57BL/6 mice, Y989-IRS-1 phosphorylation was significantly decreased and S307-IRS-1 phosphorylation significantly increased in livers of *db/db* normal and *db/db* + pcDNA mice. These changes were prevented in *db/db* mice injected with *CYP2J3*⁺. Representative Western blots are shown above graphs summarizing densitometric quantification. **P* < 0.05 versus C57BL/6; #*P* < 0.05 versus *db/db* + pcDNA; *n* = 8 per group. **B:** Levels of pS1177-eNOS in liver were lower and levels of pT495-eNOS were higher in *db/db* mice than in C57BL/6 mice. The downregulation of pS1177-eNOS was inhibited by injection with *CYP2J3*⁺, whereas no effect was observed on pT495-eNOS. Representative Western blots are shown above graphs summarizing densitometric quantification. **P* < 0.05 versus C57BL/6; #*P* < 0.05 versus *db/db* + pcDNA; *n* = 8 per group.

were reversed by *CYP2J3*⁺ treatment, these data provide further evidence that *CYP2J3* can attenuate insulin resistance in this animal model.

A glucose tolerance test was performed in C57BL/6 and *db/db* mice 2 weeks after gene delivery. Fasting plasma glucose levels before glucose loading and plasma glucose levels after glucose loading were not altered by the various gene therapy treatments in C57BL/6 mice (Fig. 3C). Compared with levels in C57BL/6 mice, fasting plasma glucose levels before glucose loading and plasma glucose levels after glucose loading were significantly higher in all *db/db* mouse groups. However, the glucose levels before and after glucose loading in *db/db* + *CYP2J3*⁺ mice were significantly lower than those in the *db/db* control and *db/db* + pcDNA groups (*P* < 0.05) (Fig. 3C). A similar profile for fasting plasma insulin levels and for plasma insulin levels after glucose loading was observed, with *db/db* + *CYP2J3*⁺ mice having levels lower than those of the other *db/db* groups but higher than those of all of the C57BL/6 groups at all time points assessed (Fig. 3D). These data indicate that *CYP2J3* gene delivery attenuated insulin resistance and has antidiabetic effects in *db/db* mice.

Effects of *CYP2J3* gene delivery on activation of mouse insulin receptor signaling and eNOS phosphorylation. Similar to the effects of fructose drinking on rats, S307 IRS-1 phosphorylation was significantly increased and Y989-IRS-1 phosphorylation was significantly decreased in livers of *db/db* control and *db/db* + pcDNA

mice relative to C57BL/6 mice (Fig. 4A). Similar effects were observed in skeletal muscle (supplementary Fig. 2A). Administration of *CYP2J3*⁺ to *db/db* mice prevented these changes in both tissues (Fig. 4A; supplementary Fig. 2A).

The effects of *CYP2J3*⁺ treatment on the phosphorylation status of eNOS were examined in liver and skeletal muscle. The level of phospho-T495-eNOS was higher but phospho-S1177-eNOS was lower in livers of *db/db* mice compared with C57BL/6 mice (Fig. 4B). *CYP2J3* gene delivery prevented the downregulation of phospho-S1177-eNOS but had no impact on phospho-T495-eNOS (Fig. 4B). Similar results were found in skeletal muscle (supplementary Fig. 3B), heart, and kidney (data not shown). These results suggest that *CYP2J3*⁺ treatment in *db/db* mice altered eNOS phosphorylation status.

Effects of *CYP2J3* gene delivery on intracellular signaling pathways in rats and mice. To investigate potential mechanisms underlying the observed effects of *CYP2J3*⁺ treatment in rats, the protein expression levels of a variety of intracellular signaling pathway molecules were investigated in liver, skeletal muscle, heart, and kidney of rats and mice in all treatment groups 2 weeks after gene delivery. The signaling molecules that were assessed included PI 3-kinase, phosphorylated AKT (P-T308-AKT), phosphorylated AMP-activated protein kinases (P-T172-AMPKs), and phosphorylated p42/44 MAPK (P-MAPK). A similar pattern of expression was observed for all four molecules in all four tissues that were examined. Specifically, tissue protein levels of the specified signaling mole-

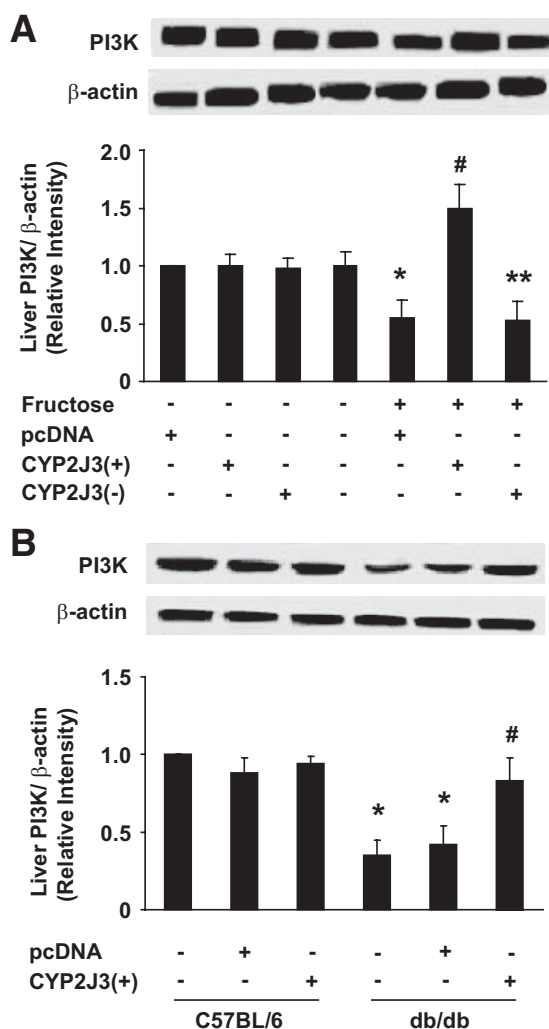


FIG. 5. Effects of *CYP2J3* gene delivery on liver PI 3-kinase (PI3K) expression in fructose-treated rats and mice. **A:** Decreased liver PI 3-kinase protein levels were observed in fructose-treated rats, and this was prevented by injection of *CYP2J3*⁺, but not by injection of *CYP2J3*⁻ or empty vector (pcDNA). **P* < 0.05 versus N + pcDNA; #*P* < 0.05 versus F + pcDNA; ***P* < 0.05 versus F + *CYP2J3*⁺; *n* = 8 per group. **B:** Liver PI 3-kinase protein levels were decreased in *db/db* mice compared with C57BL/6 mice. This decrease was prevented by injection of *CYP2J3*⁺ but not by injection of empty vector (pcDNA). **P* < 0.05 versus C57BL/6 group; #*P* < 0.05 versus *db/db* + pcDNA; *n* = 8 per group. For both **A** and **B**, representative Western blots are shown above graphs summarizing densitometric quantification.

cles were significantly decreased in fructose-treated rats and *db/db* mice compared with levels in normal water-fed rats and C57BL/6 mice, respectively. The only fructose-treated rats or *db/db* mice in which these decreases were not observed were those that had been injected with *CYP2J3*⁺. PI 3-kinase (P110) expression level data for rat and mouse liver are shown in Fig. 5A and B, whereas data for PI 3-kinase in rat and mouse liver and skeletal muscle and for P-AKT, AMPK, and P-MAPK are shown in supplementary Figs. 4–6. *CYP2J3*⁺ injection reversed changes in protein expression and phosphorylation seen in *db/db* mice or induced by fructose in rats. The notable exception to this pattern was that of P-MAPK in rat tissues, in which fructose feeding did not result in a decreased level of P-MAPK; however, *CYP2J3*⁺ injection nonetheless increased expression of P-MAPK (supplementary Fig. 6A and B). Similar results were found for all of these signaling molecules in heart and kidney of rats and mice (data not

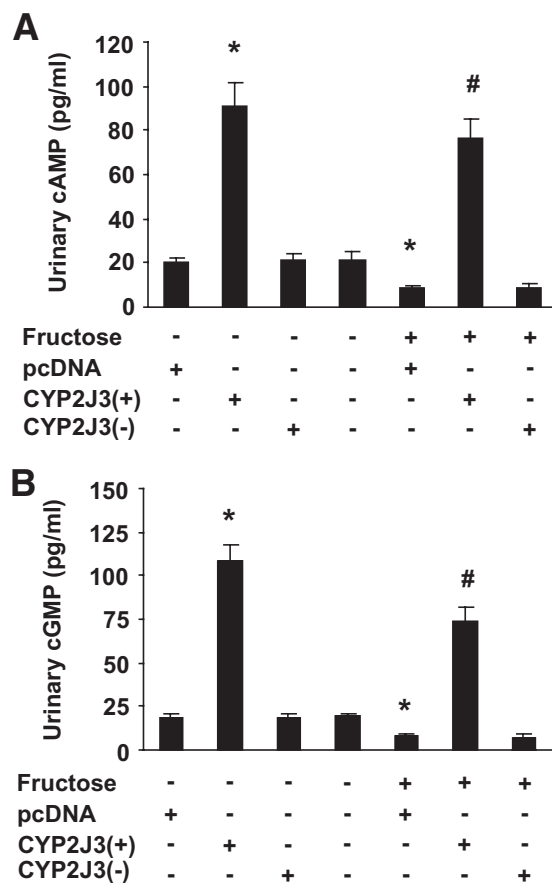


FIG. 6. Effects of *CYP2J3* gene delivery on urinary cAMP and cGMP levels. **A:** Levels of urinary cAMP were increased in rats 2 weeks after injection with *CYP2J3*⁺ compared with levels observed after injection with the empty pcDNA3.1 vector. **B:** Urinary cGMP levels were increased in rats injected with *CYP2J3*⁺ compared with those injected with the empty pcDNA vector. **P* < 0.05 versus pcDNA-treated and normal water-treated rats; #*P* < 0.05 versus pcDNA-treated and fructose-treated rats; *n* = 8 per group.

shown). These data suggest that reversal of insulin resistance by *CYP2J3*⁺ treatment was associated with restoration of these important intracellular signaling molecules to normal levels.

Effects of *CYP2J3* gene delivery on urinary cAMP and cGMP levels. To investigate potential mechanisms underlying the observed effects of *CYP2J3* on the upregulation of AMPK phosphorylation, cAMP and cGMP levels were determined in urine of rats in all treatment groups 2 weeks after gene delivery. Compared with rats treated with normal water, the concentration of urinary cAMP and cGMP decreased significantly in rats with fructose water treatment. Interestingly, *CYP2J3* gene delivery significantly increased urinary cAMP and cGMP level in rats treated with both normal water and fructose water (Fig. 6A and B). These data indicate that *CYP2J3* overexpression induced a significant increase in urine cAMP and cGMP secretion, which may result from G-protein-coupled receptor (GPCR) activation by EETs.

DISCUSSION

This study was undertaken to examine the effects of *CYP2J3* gene delivery on insulin resistance and diabetes in fructose-induced insulin-resistant rats and *db/db* diabetic mice. Results showed that a single intravenous injection of *CYP2J3* in the eukaryotic expression plasmid pcDNA

reduced blood pressure in fructose-fed rats and improved sensitivity to insulin in peripheral tissues and organs in both animal models. *CYP2J3* overexpression significantly reduced blood pressure with upregulated eNOS expression and downregulated ET-1 and ETA expression. Furthermore, *CYP2J3* overexpression significantly improved insulin resistance in fructose-induced insulin-resistant rats and *db/db* diabetic mice, at least in part through eNOS, IRS-1, and PI 3-kinase/AKT signaling pathways, as well as AMPK signaling pathways in liver, muscle, heart, and kidney. These data provide direct evidence that *CYP2J3*-derived EETs may alleviate insulin resistance through a variety of beneficial effects on critical intracellular signaling pathways.

Previous studies have demonstrated that rats treated with high-fructose drinking water develop systemic hypertension, hyperinsulinemia, and hypertriglyceridemia (24). Although the pathophysiological mechanisms responsible for elevated blood pressure and hyperinsulinemia in fructose-treated animals are not completely understood, elevated sympathetic nervous system activity, impaired endothelium-dependent dilation, reduction of capillary permeability, elevated vascular expression of ET-1 and ETA receptor genes, decreased eNOS activity, and increased salt absorption by the intestine and kidney have all been implicated (12,23,25). Polymorphisms in *CYP2J2* (the human homolog of *CYP2J3*) have been associated with essential hypertension (26), and reduced renal CYP-derived eicosanoid synthesis has been reported in rats with high-fat diet-induced hypertension (27). Furthermore, EETs have direct vasodilatory activity (28,29). In the present study, *CYP2J3* overexpression significantly elevated urinary levels of 14,15-DHET in rats and mice and attenuated fructose-induced changes in eNOS, ET-1, and ETA-R expression in rats. These effects may underlie the beneficial effects of *CYP2J3* overexpression on blood pressure and hyperinsulinemia that we observed.

Fructose induces inflammatory changes in human aortic endothelial cells and vessel walls in rats (30,31). Cytokines such as TNF- α induce insulin resistance in endothelial cells via a p38 mitogen-activated protein kinase-dependent pathway (32). This inflammatory signaling is relevant to diabetes, as TNF receptor 1 blockade protects Wistar rats from diet-induced obesity and insulin resistance (33). Physiological concentrations of EETs or overexpression of *CYP2J2* decreases cytokine-induced endothelial cell adhesion molecule expression, indicating that EETs have anti-inflammatory properties independent of their membrane-hyperpolarizing effects (34). Furthermore, increased NO release improves insulin resistance in fructose-treated rats (23,35). Potassium depletion in rats exacerbates endothelial dysfunction and lowers the bioavailability of NO, which blocks insulin activity and causes insulin resistance (35). We observed that *CYP2J3* expression resulted in a significant reduction in urine volume and urine potassium in fructose-treated rats. This suggests a potential ameliorative effect of *CYP2J3* treatment against hypertension-related end organ (kidney) damage and attenuation of insulin resistance.

The precise molecular mechanisms for attenuation of insulin resistance in *CYP2J3*-injected, fructose-treated rats remain to be elucidated. Recent studies indicate that the ability of insulin to vasodilate skeletal muscle vasculature is mediated by endothelium-derived NO (36). These actions may partially explain our observation of improved insulin sensitivity after *CYP2J3* gene delivery. In addition,

we observed effects on insulin signaling in tissues directly involved in insulin sensitivity (37–40), including liver, muscle, heart, and kidney, as well as in an islet cell line. Our data show that insulin-dependent signaling was significantly inhibited in fructose-treated rats and *db/db* mice, but dramatically reversed by *CYP2J3* overexpression. These results indicate that *CYP2J3* overexpression potentiates insulin receptor signaling in liver, muscle, heart, and kidney and thus improves insulin sensitivity.

We also evaluated the phosphorylation status of AMPK. Small molecule-mediated activation of AMPK improves insulin resistance in *ob/ob* mice (41) and represents a promising approach for the treatment of type 2 diabetes and metabolic syndrome (42). We found that *CYP2J3* overexpression resulted in a significant increase in AMPK phosphorylation, which may contribute to the EET-mediated alleviation of diabetes and insulin resistance we observed. *CYP2J3* overexpression induced a significant increase in urine cAMP and cGMP secretion, which may result from GPCR activation by EETs. Thus, EET-induced GPCR activation may play an important role in EET-mediated AMPK activation and insulin sensitization. Taken together, these data suggest that the improvement of insulin resistance after *CYP2J3* gene delivery was due to, at least in part, increased activation of IR/IRS-1/PI 3-kinase/AKT and AMPK signaling pathways (43), as well as the upregulation of eNOS.

In conclusion, we have demonstrated alleviation of insulin resistance and diabetes by *CYP2J3* gene therapy in *db/db* diabetic mice and a model of fructose-induced insulin resistance in rats. These effects were associated with increased insulin sensitivity in peripheral tissues and organs via upregulation of systemic eNOS and activation of the IRS-1/PI 3-kinase/AKT and AMPK signaling pathways in muscle, liver, heart, kidney, and aorta. However, the more precise mechanisms need to be further investigated. The ability of CYP epoxygenase delivery to exert a broad spectrum of beneficial effects in these animal models warrants further investigation of this approach in the treatment of hypertension associated with insulin resistance and diabetes in humans.

ACKNOWLEDGMENTS

This work was supported in part by funds from the National Education Ministration project, Nature Science Foundation Committee projects (Nos. 30930039 and 30700377), Wuhan project (200870834407), 973 program (2007CB512004), and the Intramural Research Program of the National Institutes of Health, National Institute of Environmental Health Sciences.

No potential conflicts of interest relevant to this article were reported.

We thank Dr. Jeffrey Card for assistance with the editing of this article. We also thank Dr. Stavros Garantziotis and Michael Fessler for helpful comments during the preparation of this article.

REFERENCES

1. Wu S, Moomaw CR, Tomer KB, Falck JR, Zeldin DC. Molecular cloning and expression of CYP2J2, a human cytochrome P450 arachidonic acid epoxygenase highly expressed in heart. *J Biol Chem* 1996;271:3460–3468
2. Zeldin DC, Foley J, Boyle JE, Moomaw CR, Tomer KB, Parker C, Steenbergen C, Wu S. Predominant expression of an arachidonate epoxygenase in islets of Langerhans cells in human and rat pancreas. *Endocrinology* 1997;138:1338–1346
3. Zeldin DC, Foley J, Goldsworthy SM, Cook ME, Boyle JE, Ma J, Moomaw

- CR, Tomer KB, Steenbergen C, Wu S. CYP2J subfamily cytochrome P450s in the gastrointestinal tract: expression, localization, and potential functional significance. *Mol Pharmacol* 1997;51:931-943
4. Wu S, Chen W, Murphy E, Gabel S, Tomer KB, Foley J, Steenbergen C, Falck JR, Moomaw CR, Zeldin DC. Molecular cloning, expression, and functional significance of a cytochrome P450 highly expressed in rat heart myocytes. *J Biol Chem* 1997;272:12551-12559
 5. Wang Y, Wei X, Xiao X, Hui R, Card JW, Carey MA, Wang DW, Zeldin DC. Arachidonic acid epoxygenase metabolites stimulate endothelial cell growth and angiogenesis via mitogen-activated protein kinase and phosphatidylinositol 3-kinase/Akt signaling pathways. *J Pharmacol Exp Ther* 2005;314:522-532
 6. Wang H, Lin L, Jiang J, Wang Y, Lu ZY, Bradbury JA, Lih FB, Wang DW, Zeldin DC. Up-regulation of endothelial nitric-oxide synthase by endothelium-derived hyperpolarizing factor involves mitogen-activated protein kinase and protein kinase C signaling pathways. *J Pharmacol Exp Ther* 2003;307:753-764
 7. Jiang JG, Chen CL, Card JW, Yang S, Chen JX, Fu XN, Ning YG, Xiao X, Zeldin DC, Wang DW. Cytochrome P450 2J2 promotes the neoplastic phenotype of carcinoma cells and is up-regulated in human tumors. *Cancer Res* 2005;65:4707-4715
 8. Yang S, Lin L, Chen JX, Lee CR, Seubert JM, Wang Y, Wang H, Chao ZR, Tao DD, Gong JP, Lu ZY, Wang DW, Zeldin DC. Cytochrome P-450 epoxygenases protect endothelial cells from apoptosis induced by tumor necrosis factor-alpha via MAPK and PI3K/Akt signaling pathways. *Am J Physiol Heart Circ Physiol* 2007;293:H1142-H1151
 9. Hercule HC, Schunck WH, Gross V, Seringer J, Leung FP, Weldon SM, da Costa Goncalves ACh, Huang Y, Luft FC, Gollasch M. Interaction between P450 eicosanoids and nitric oxide in the control of arterial tone in mice. *Arterioscler Thromb Vasc Biol* 2009;29:54-60
 10. Desjardins F, Balligand JL. Nitric oxide-dependent endothelial function and cardiovascular disease. *Acta Clin Belg* 2006;61:326-334
 11. Huang PL, Huang Z, Mashimo H, Bloch KD, Moskowitz MA, Bevan JA, Fishman MC. Hypertension in mice lacking the gene for endothelial nitric oxide synthase. *Nature* 1995;377:239-242
 12. Miatello R, Risler N, Castro C, González S, Rüttler M, Cruzado M. Aortic smooth muscle cell proliferation and endothelial nitric oxide synthase activity in fructose-fed rats. *Am J Hypertens* 2001;14:1135-1141
 13. Alexander MY, Brosnan MJ, Hamilton CA, Downie P, Devlin AM, Dowell F, Martin W, Prentice HM, O'Brien T, Dominiczak AF. Gene transfer of endothelial nitric oxide synthase improves nitric oxide-dependent endothelial function in a hypertensive rat model. *Cardiovasc Res* 1999;43:798-807
 14. Alexander MY, Brosnan MJ, Hamilton CA, Fennell JP, Beattie EC, Jardine E, Heistad DD, Dominiczak AF. Gene transfer of endothelial nitric oxide synthase but not Cu/Zn superoxide dismutase restores nitric oxide availability in the SHRSP. *Cardiovasc Res* 2000;47:609-617
 15. Guzik TJ, Mussa S, Gastaldi D, Sadowski J, Ratnatunga C, Pillai R, Channon KM. Mechanisms of increased vascular superoxide production in human diabetes mellitus: role of NAD(P)H oxidase and endothelial nitric oxide synthase. *Circulation* 2002;105:1656-1662
 16. Satoh M, Fujimoto S, Haruna Y, Arakawa S, Horike H, Komai N, Sasaki T, Tsujioka K, Makino H, Kashihara N. NAD(P)H oxidase and uncoupled nitric oxide synthase are major sources of glomerular superoxide in rats with experimental diabetic nephropathy. *Am J Physiol Renal Physiol* 2005;288:F1144-F1152
 17. Toutouzas K, Riga M, Stefanadi E, Stefanadis C. Asymmetric dimethylarginine (ADMA) and other endogenous nitric oxide synthase (NOS) inhibitors as an important cause of vascular insulin resistance. *Horm Metab Res* 2008;40:655-659
 18. Sowers JR. Insulin resistance and hypertension. *Am J Physiol Heart Circ Physiol* 2004;286:H1597-H1602
 19. Zhao C, Wang P, Xiao X, Chao J, Wang DW, Zeldin DC. Gene therapy with human tissue kallikrein reduces hypertension and hyperinsulinemia in fructose-induced hypertensive rats. *Hypertension* 2003;42:1026-1033
 20. Schneemann A, Dijkstra BG, van den Berg TJ, Kamphuis W, Hoyng PF. Nitric oxide/guanylate cyclase pathways and flow in anterior segment perfusion. *Graefes Arch Clin Exp Ophthalmol* 2002;240:936-941
 21. Tu L, Xu X, Wan H, Zhou C, Deng J, Xu G, Xiao X, Chen Y, Edin ML, Voltz JW, Zeldin DC, Wang DW. Delivery of recombinant adeno-associated virus-mediated human tissue kallikrein for therapy of chronic renal failure in rats. *Human Gene Ther* 2008;19:318-330
 22. Virkamäki A, Ueki K, Kahn CR. Protein-protein interaction in insulin signaling and the molecular mechanisms of insulin resistance. *J Clin Invest* 1999;103:931-943
 23. Zhao CX, Xu X, Cui Y, Wang P, Wei X, Yang S, Edin ML, Zeldin DC, Wang DW. Increased endothelial nitric-oxide synthase expression reduces hypertension and hyperinsulinemia in fructose-treated rats. *J Pharmacol Exp Ther* 2009;328:610-620
 24. Thorburn AW, Storlien LH, Jenkins AB, Khouri S, Kraegen EW. Fructose-induced in vivo insulin resistance and elevated plasma triglyceride levels in rats. *Am J Clin Nutr* 1989;49:1155-1163
 25. Singh AK, Amlal H, Haas PJ, Dringenberg U, Fussell S, Barone SL, Engelhardt R, Zuo J, Seidler U, Soleimani M. Fructose-induced hypertension: essential role of chloride and fructose absorbing transporters PAT1 and Glut5. *Kidney Int* 2008;74:438-447
 26. Wu SN, Zhang Y, Gardner CO, Chen Q, Li Y, Wang GL, Gao PJ, Zhu DL. Evidence for association of polymorphisms in CYP2J2 and susceptibility to essential hypertension. *Ann Intern Med* 2007;71:519-525
 27. Wang MH, Smith A, Zhou Y, Chang HH, Lin S, Zhao X, Imig JD, Dorrance AM. Downregulation of renal CYP-derived eicosanoid synthesis in rats with diet-induced hypertension. *Hypertension* 2003;42:594-599
 28. Campbell WB, Gebremedhin D, Pratt PF, Harder DR. Identification of epoxyeicosatrienoic acids as endothelium-derived hyperpolarizing factors. *Circ Res* 1996;78:415-423
 29. McGiff JC. Cytochrome P-450 metabolism of arachidonic acid. *Annu Rev Pharmacol Toxicol* 1991;31:339-369
 30. Glushakova O, Kosugi T, Roncal C, Mu W, Heinig M, Cirillo P, Sánchez-Lozada LG, Johnson RJ, Nakagawa T. Fructose induces the inflammatory molecule ICAM-1 in endothelial cells. *J Am Soc Nephrol* 2008;19:1712-1720
 31. Tan HW, Xing SS, Bi XP, Li L, Gong HP, Zhong M, Zhang Y, Zhang W. Felodipine attenuates vascular inflammation in a fructose-induced rat model of metabolic syndrome via the inhibition of NF-kappaB activation. *Acta Pharmacol Sin* 2008;29:1051-1059
 32. Li G, Barrett EJ, Barrett MO, Cao W, Liu Z. Tumor necrosis factor-alpha induces insulin resistance in endothelial cells via a p38 mitogen-activated protein kinase-dependent pathway. *Endocrinology* 2007;148:3356-3363
 33. Liang H, Yin B, Zhang H, Zhang S, Zeng Q, Wang J, Jiang X, Yuan L, Wang CY, Li Z. Blockade of tumor necrosis factor (TNF) receptor type 1-mediated TNF-alpha signaling protected Wistar rats from diet-induced obesity and insulin resistance. *Endocrinology* 2008;149:2943-2951
 34. Node K, Huo Y, Ruan X, Yang B, Spiecker M, Ley K, Zeldin DC, Liao JK. Anti-inflammatory properties of cytochrome P450 epoxygenase-derived eicosanoids. *Science* 1999;285:1276-1279
 35. Reungjui S, Roncal CA, Mu W, Srinivas TR, Sirivongs D, Johnson RJ, Nakagawa T. Thiazide diuretics exacerbate fructose-induced metabolic syndrome. *J Am Soc Nephrol* 2007;18:2724-2731
 36. Steinberg HO, Brechtel G, Johnson A, Fineberg N, Baron AD. Insulin-mediated skeletal muscle vasodilation is nitric oxide dependent: a novel action of insulin to increase nitric oxide release. *J Clin Invest* 1994;94:1172-1179
 37. Björnholm M, Kawano Y, Lehtihet M, Zierath JR. Insulin receptor substrate-1 phosphorylation and phosphatidylinositol 3-kinase activity in skeletal muscle from NIDDM subjects after in vivo insulin stimulation. *Diabetes* 1997;46:524-527
 38. Kim YB, Nikoulina SE, Ciaraldi TP, Henry RR, Kahn BB. Normal insulin-dependent activation of Akt/protein kinase B, with diminished activation of phosphoinositide 3-kinase, in muscle in type 2 diabetes. *J Clin Invest* 1999;104:733-741
 39. Kohn AD, Summers SA, Birnbaum MJ, Roth RA. Expression of a constitutively active Akt Ser/Thr kinase in 3T3-L1 adipocytes stimulates glucose uptake and glucose transporter 4 translocation. *J Biol Chem* 1996;271:31372-31378
 40. Li P, Koike T, Qin B, Kubota M, Kawata Y, Jia YJ, Oshida Y. A high-fructose diet impairs Akt and PKCzeta phosphorylation and GLUT4 translocation in rat skeletal muscle. *Horm Metab Res* 2008;40:528-532
 41. Watanabe T, Kubota N, Ohsugi M, Kubota T, Takamoto I, Iwabu M, Awazawa M, Katsuyama H, Hasegawa C, Tokuyama K, Moroi M, Sugi K, Yamauchi T, Noda T, Nagai R, Terauchi Y, Tobe K, Ueki K, Kadowaki T. Rimonabant ameliorates insulin resistance via both adiponectin-dependent and adiponectin-independent pathways. *J Biol Chem* 2009;284:1803-1812
 42. Cool B, Zinker B, Chiou W, Kifle L, Cao N, Perham M, Dickinson R, Adler A, Gagne G, Iyengar R, Zhao G, Marsh K, Kym P, Jung P, Camp HS, Frevert E. Identification and characterization of a small molecule AMPK activator that treats key components of type 2 diabetes and the metabolic syndrome. *Cell Metab* 2006;3:403-416
 43. Hutchinson DS, Summers RJ, Bengtsson T. Regulation of AMP-activated protein kinase activity by G-protein coupled receptors: potential utility in treatment of diabetes and heart disease. *Pharmacol Ther* 2008;119:291-310